

Supporting Information for
“Comment on ‘Aggregation-induced phosphorescent emission (AIPE) of
iridium(III) complexes’: origin of the enhanced phosphorescence”

Youngmin You^a, Hyun Sue Huh^b, Kil Suk Kim^c, Soon Won Lee^b, Dongho Kim^c, and Soo Young Park^{a}*

^a *Department of Materials Science & Engineering, Seoul National University, San 56-1, Shillim-Dong, Kwanak-Gu, Seoul 151-744, Korea*

^b *Department of Chemistry, Sungkyunkwan University, Natural Science Campus 330416, Suwon 440-746, Korea*

^c *Department of Chemistry, Yonsei University, Seoul 120-749, Korea*

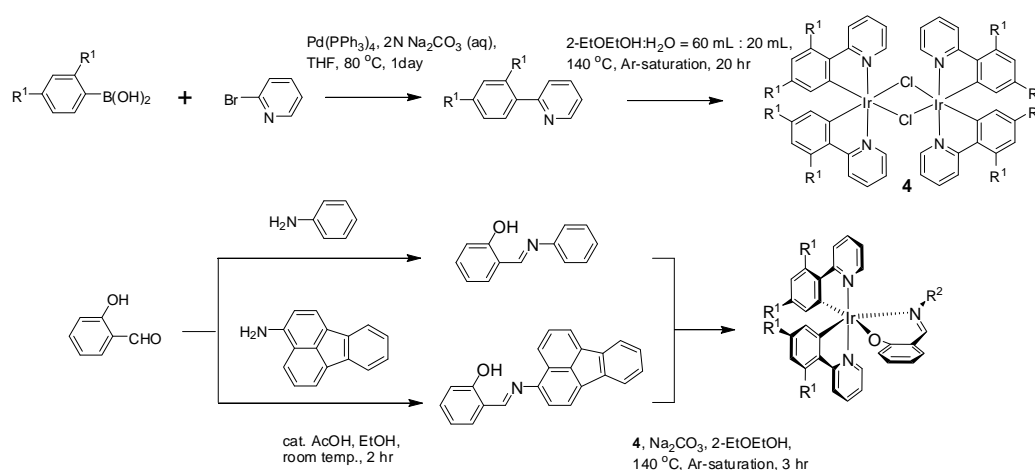
Email: parksy@snu.ac.kr

List of Supporting Information

1. Synthetic details and characterization
2. **SI 1.** Absorption and phosphorescence spectra of **2–4**.
3. **SI 2.** Comparative view of the absorption (CH_2Cl_2 , 10 μM) and phosphorescence (PMMA film, 2 wt%) spectra of **1–4**.
4. **SI 3.** Evolution of phosphorescence spectra of **1** (CHCl_3 , 10 μM) as a function of temperature.
5. **SI 4.** Change in phosphorescence of the film states of **1** of neat film, PMMA film (2 wt%), PS film (2 wt%), and PBMA film (2 wt%), respectively.
6. **SI 5.** Change in phosphorescence of the film states of **2** (top) and **3** (down) of PMMA film, PS film, and PBMA film, respectively (2 wt% each).
7. **SI 6.** A plot of $\ln(1/t_p)$ (t_p : phosphorescence lifetime) as a function of $1/T$ (T: temperature, K) of a PMMA film doped with **1** (2 wt%).
8. **SI 7.** Orbital configurations constituting triplet states designated in Fig. 4 of main text.
9. **SI 8.** (a) LUMO (top, UHF/lanl2dz) and the crystal structure geometry (bottom) of **1**. (b) LUMO (top) and the optimized geometry (bottom) of the triplet state of **1** (UCIS/lanl2dz).

1. Synthetic details and characterization

Materials. Materials obtained from commercial supplier were used without further purification unless otherwise stated. All glasswares, syringes, magnetic stirring bars, and needles were dried in the convection oven at least 4 hours. Reactions were monitored with thin layer chromatography (TLC). Commercial TLC plates (silica gel 60 F₂₅₄, Merck Co.) were developed and the spots were seen under UV light at 254 and 365 nm, or stained with *p*-anisaldehyde. Silica column chromatography was done with silica gel 60 G (particle size 5-40 μm, Merck Co.). Synthetic scheme for the Ir(III) complexes is shown in Scheme 1. 2-(2,4-Difluorophenyl)pyridine (*dfppy*), [(*dfppy*)₂Ir(μ-Cl)]₂, 2-phenylpyridine (*ppy*), and [(*ppy*)₂Ir(μ-Cl)]₂ were synthesized according to literature procedure.¹ Poly(methylmethacrylate), poly(butylmethacrylate) and poly(styrene) were purchased from Aldrich, which were further purified through repeated reprecipitations (CHCl₃/MeOH).



Scheme 1. Synthesis of the Ir(III) complexes.

2-((Phenylimino)methyl)phenol. A EtOH solution (8.0 mL) dissolved by salicylaldehyde (2.3 mL, 22 mmol) was added to a stirred EtOH solution (40 mL) of aniline (2.0 mL, 22 mmol). After adding catalytic amount of AcOH, the reaction mixture was stirred at room temperature for 2 hr. Concentration and subsequent silica gel column purification gave yellow liquid (4.12 g, 20.9 mmol) in 95% yield. ¹H NMR (500 MHz, CDCl₃) δ: 6.87 (t, 1H, *J* = 7.6 Hz), 6.99 (d, *J* = 8.2 Hz, 1H), 7.21 (m, 3H), 7.30 (d, *J* = 7.5 Hz, 2H), 7.35 (t, *J* = 7.5 Hz, 2H), 8.50 (s, 1H), 13.3 (s, 1H). ¹³C NMR (125 MHz, CDCl₃) δ: 117.29, 119.11, 119.28, 121.25, 126.97, 129.45, 132.40, 133.18, 148.37, 161.23, 162.69. HRMS (EI, DIP) *m/z*: calcd for C₁₃H₁₁NO, 197.0841; found, 197.0844. Anal. Calcd for C₁₃H₁₁NO: C, 79.16; H, 5.62; N, 7.10. Found: C, 78.96; H, 5.57; N, 7.06.

2-((Fluoranthen-3-ylimino)methyl)phenol. Same procedure of 2-((Phenylimino)methyl)phenol was applied for this synthesis to give orange powder (0.666 g, 2.97 mmol) in 45% yield. ¹H NMR (500 MHz, CDCl₃) δ: 6.96 (d, *J* = 7.6 Hz, 1H), 7.09 (d, *J* = 8.6 Hz, 1H), 7.25 (d, *J* = 7.3 Hz, 1H), 7.35 (m, 2H), 7.42 (m, 2H), 7.62 (t, *J* = 7.0 Hz, 1H), 7.84 (m, 3H), 7.92 (d, *J* = 6.8 Hz, 1H), 8.08 (d, *J* = 8.3 Hz, 1H), 8.70 (s, 1H), 13.35 (s, 1H). ¹³C NMR (125 MHz, CDCl₃) δ: 116.04, 117.55, 119.45, 119.66, 120.76, 120.88, 121.60, 121.84, 123.18, 125.67, 127.64,

127.89, 128.57, 132.68, 133.31, 133.72, 135.99, 136.95, 139.12, 139.82, 146.20, 161.59, 163.59. HRMS (EI, DIP) m/z : calcd for $C_{23}H_{15}NO$, 321.1154; found, 321.1150. Anal. Calcd for $C_{23}H_{15}NO$: C, 85.96; H, 4.70; N, 4.36. Found: C, 85.94; H, 4.71; N, 4.32.

Iridium (III) bis(2-(2,4-difluorophenyl)pyridinato- $N,C^{2'}$) (2-((phenylimino)methyl)phenolate) (1). $[(Dfppy)_2Ir(\mu-Cl)]_2$ (0.400 g, 0.330 mmol), sodium carbonate (0.279 g, 2.63 mmol), and 2-((phenylimino)methyl)phenol (0.389 g, 1.97 mmol) were dissolved in 30 mL of 2-EtOEtOH. After degassing, the reaction vessel was maintained under Ar condition. Temperature was raised to 140 °C and the reaction mixture was stirred for 3 h. The cooled crude mixture was poured to EtOAc (150 mL), and extracted with water (100 mL \times three times) to remove 2-EtOEtOH. Silica column purification with n -hexane:EtOAc = 4:1 and reprecipitation in ether: n -hexane = 10 mL:40 mL gave a yellow powder (0.368 g, 0.470 mmol) in 71% yield. TLC, R_f = 0.3 (n -hexane:EtOAc = 4:1). 1H NMR δ : 5.60 (dd, J = 2.3, 8.9 Hz, 1H), 5.66 (dd, J = 2.4, 8.9 Hz, 1H), 6.06 (m, 1H), 6.10 (m, 2H), 6.35 (m, 1H), 6.42 (t, J = 7.83 Hz, 1H), 6.69 (d, J = 8.5 Hz, 1H), 6.80 (m, 2H), 6.89 (d, J = 6.0 Hz, 1H), 7.08 (m, 2H), 7.18 (td, J = 5.9 Hz, 1H), 7.22 (m, 1H), 7.75 (q, J = 7.7 Hz, 2H), 7.93 (d, J = 8.4 Hz, 1H), 8.07 (s, 1H), 8.28 (d, J = 8.3 Hz, 1H), 8.82 (d, J = 5.8 Hz, 1H), 8.88 (d, J = 5.8 Hz, 1H). ^{13}C NMR (125 MHz, $CDCl_3$) δ : 102.7, 112.0, 116.2, 118.5, 118.7, 120.8, 121.0, 121.4, 122.0, 122.1, 122.2, 122.5, 122.8, 124.2, 124.3, 127.2, 130.0, 130.1, 130.5, 130.8, 132.1, 132.4, 137.2, 137.3, 150.1, 150.2, 152.0, 157.4, 157.5, 157.8, 160.0, 160.1, 160.2, 163.1. FAB-MS (DIP) m/z 783 (M^+). Anal. Calcd for $C_{35}H_{22}F_4IrN_3O$: C, 55.16; H, 3.21; N, 5.36. Found: C, 55.06; H, 3.21; N, 5.34.

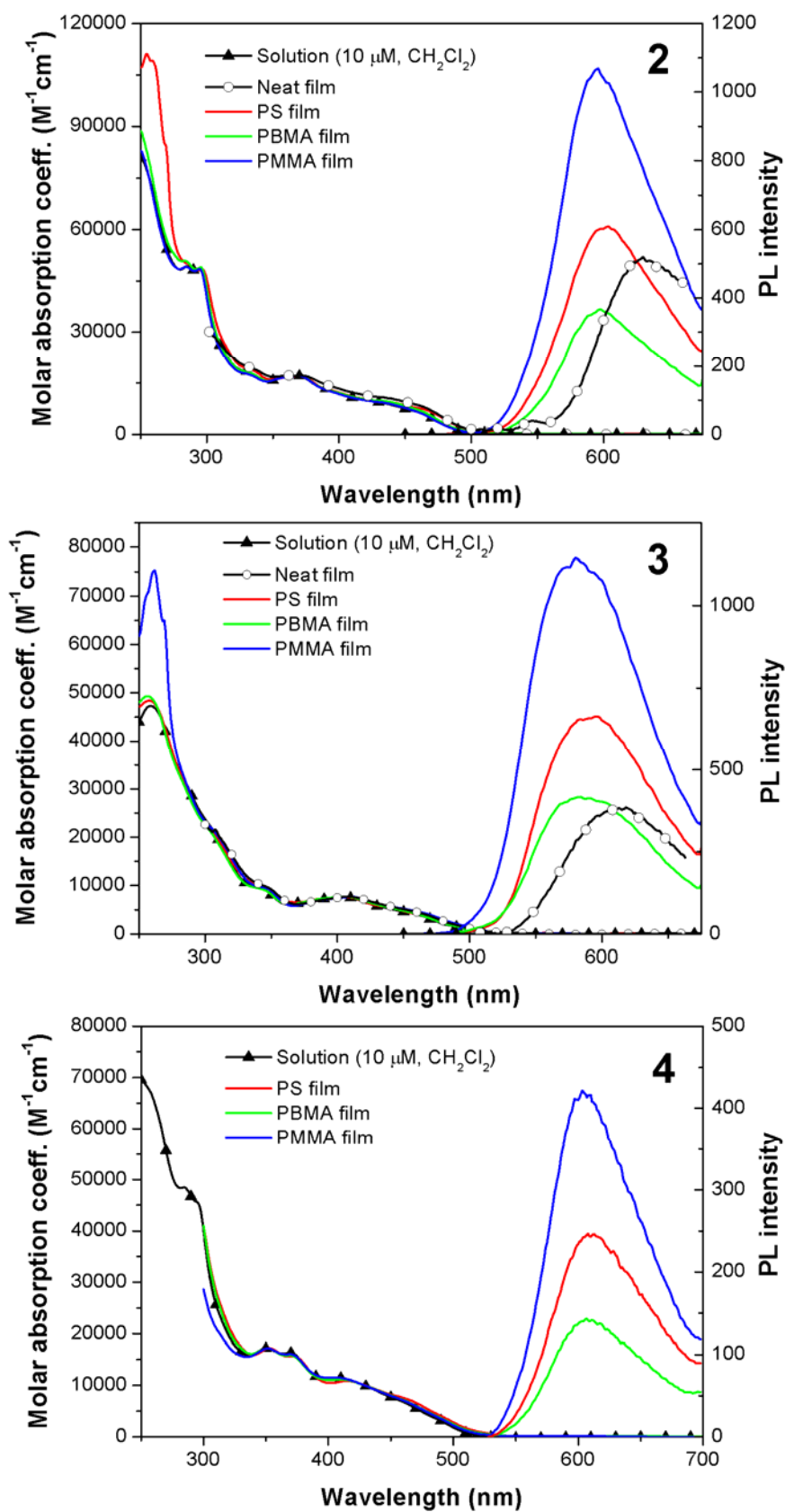
Iridium (III) bis(2-(2,4-difluorophenyl)pyridinato- $N,C^{2'}$) (2-((fluoranthen-3-ylimino)methyl)phenolate) (2). Same method for **1** was applied to give red powder (0.201 g, 0.221 mmol) in 41%. TLC, R_f = 0.4 (n -hexane:EtOAc = 2:1). 1H NMR δ : 5.59 (d, J = 8.5 Hz, 1H), 5.64 (d, J = 8.7 Hz, 1H), 5.87 (t, J = 8.1 Hz, 1H), 6.35 (t, J = 8.0 Hz, 1H), 6.45 (t, J = 6.1 Hz, 1H), 6.60 (d, J = 8.3 Hz, 1H), 6.87 (m, 2H), 7.01 (t, J = 6.0 Hz, 1H), 7.12 (m, 3H), 7.24–7.38 (broad m, 7H), 7.70 (d, J = 6.9 Hz, 1H), 7.75 (m, 2H), 7.81 (d, J = 7.9 Hz, 1H), 8.23 (s, 1H), 8.28 (d, J = 8.5 Hz, 1H), 9.00 (d, J = 5.5 Hz, 2H). ^{13}C NMR (125 MHz, $CDCl_3$) δ : 102.8, 112.1, 117.4, 118.5, 119.2, 120.8, 121.3, 121.4, 121.5, 121.6, 121.8, 124.1, 124.2, 128.5, 130.0, 130.1, 130.6, 130.9, 132.2, 132.7, 133.5, 134.7, 135.9, 136.2, 136.5, 136.9, 137.0, 137.2, 137.3, 139.3, 139.5, 144.4, 145.1, 147.4, 148.5, 149.5, 150.1, 150.6, 152.5, 157.4, 157.4, 157.9, 160.0, 160.2, 163.3. FAB-MS (DIP) m/z 907 ($M^+ - 1$). Anal. Calcd for $C_{40}H_{29}F_4IrN_3O$: C, 60.85; H, 3.22; N, 4.63. Found: C, 60.82; H, 3.21; N, 4.63.

Iridium (III) bis(2-phenylpyridinato- $N,C^{2'}$) (2-((phenylimino)methyl)phenolate) (3). Same method for **1** instead using $[(ppy)_2Ir(\mu-Cl)]_2$ was applied to give orange powder. 1H NMR δ : 6.13 (d, J = 7.8 Hz, 2H), 6.15 (d, J = 8.0 Hz, 1H), 6.26 (d, J = 7.5 Hz, 1H), 6.39 (t, J = 7.6 Hz, 1H), 6.49 (t, J = 7.4 Hz, 1H), 6.53 (t, J = 7.6 Hz, 1H), 6.71 (m, 4H), 6.80 (d, J = 7.3 Hz, 1H), 6.83 (t, J = 7.5 Hz, 1H), 7.03 (m, 2H), 7.11 (m, 2H), 7.22 (m, 1H), 7.51 (d, J = 7.5 Hz, 1H), 7.57 (d, J = 7.7 Hz, 1H), 7.66 (m, 2H), 7.85 (d, J = 8.1 Hz, 1H), 8.10 (s, 1H), 8.85 (d, J = 5.6 Hz, 1H), 8.91 (d, J = 5.6 Hz, 1H). ^{13}C NMR (125 MHz, $CDCl_3$) δ : 113.7, 118.0, 119.1, 119.8, 121.4, 121.7, 122.4, 122.5, 122.6, 123.6, 124.0, 124.8, 124.9, 127.6, 127.7, 127.8, 129.0, 129.6, 132.8, 133.4, 134.4, 135.4, 136.8, 136.9, 144.3, 144.8, 148.6, 149.5, 150.5, 152.0, 152.4, 161.8, 167.1, 168.8, 169.1. FAB-MS (DIP) m/z 711 ($M^+ - 1$). Anal. Calcd for $C_{36}H_{29}IrN_3O$: C, 60.74; H, 4.11; N, 5.90. Found: C, 60.72; H, 4.07; N, 5.73.

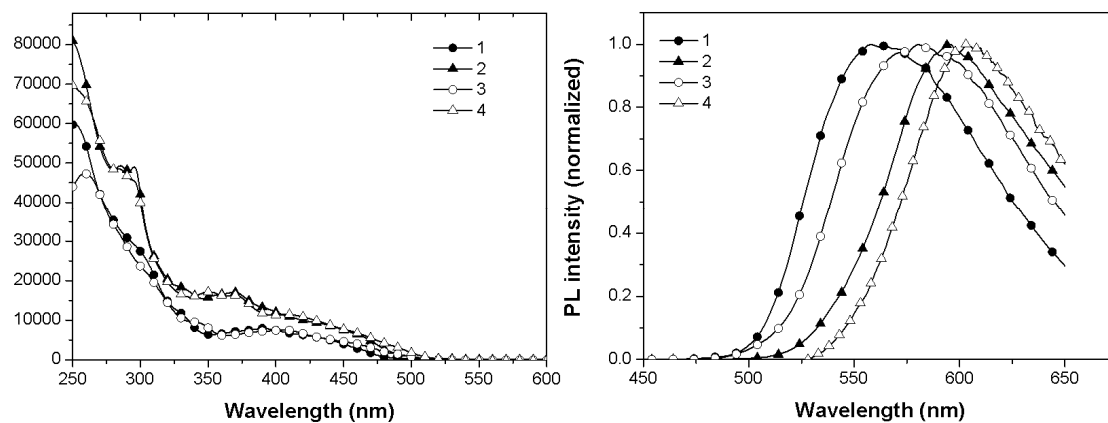
Iridium (III) bis(2phenylpyridinato-*N,C*^{2'}) (2-((fluoranthen-3-ylimino)methyl)phenolate) (4). Same method for **1** instead using [(ppy)₂Ir(μ-Cl)]₂ was applied to give orange powder. ¹H NMR δ: 6.20 (t, *J* = 6.6 Hz, 2H), 6.32 (t, *J* = 7.8 Hz, 1H), 6.42 (t, *J* = 7.0 Hz, 1H), 6.50 (m, 2H), 6.68 (t, *J* = 6.7 Hz, 1H), 6.76 (m, 3H), 6.84 (m, 2H), 7.05 (t, *J* = 7.1 Hz, 1H), 7.11 (m, 3H), 7.26 (m, 1H), 7.28 (m, 1H), 7.33 (m, 3H), 7.60 (d, *J* = 7.7 Hz, 1H), 7.71 (d, *J* = 6.9 Hz, 1H), 7.74 (m, 3H), 7.83 (d, *J* = 8.3 Hz, 1H), 7.91 (d, *J* = 8.1 Hz, 1H), 8.26 (s, 1H), 9.04 (d, *J* = 5.6 Hz, 2H). ¹³C NMR (125 MHz, CDCl₃) δ: 113.8, 117.8, 119.2, 119.4, 119.9, 121.3, 121.3, 121.4, 121.5, 121.6, 121.7, 121.8, 122.1, 123.3, 124.1, 125.1, 125.2, 127.1, 127.2, 127.7, 127.8, 129.2, 129.6, 131.8, 132.7, 133.3, 134.7, 135.8, 136.4, 136.7, 136.9, 137.0, 139.3, 139.5, 144.1, 144.8, 147.4, 148.5, 149.5, 150.6, 152.3, 163.9, 167.6, 168.4, 169.2. FAB-MS (DIP) *m/z* 836 (M⁺-1). Anal. Calcd for C₄₆H₃₃IrN₃O: C, 66.09; H, 3.98; N, 5.03. Found: C, 66.08; H, 3.99; N, 5.06.

Characterization. ¹H and ¹³C nuclear magnetic resonance (NMR) spectra were obtained in CDCl₃ at 300 MHz instrument (JEOL, JNM-LA 300 or Bruker, Avance DPX-300). Chemical shifts were recorded by ppm. Multiplicity was denoted by s (singlet), d (doublet), t (triplet), dd (doublet of doublet), m (multiplet) and br (broad). Coupling constants (*J*) were in hertz (Hz). Mass spectra (MS) were obtained with JEOL, JMS-AX505WA. Elemental analysis (EA) was performed with CE Instrument, EA1110. Absorption spectra of solution and films (spin-coated films on precleaned quartz substrates under 2000 rpm with 5 wt % solution in 1,2-dichloroethane) were recorded with SHIMAZU UV-1650PC from 280 to 700 nm. Photoluminescence spectra were obtained with a SHIMAZU RF 5301 PC spectrophotometer in the range of 400 ~ 700 nm. Ar-saturated 10 μM solution was prepared for measuring absorption and PL spectra. For the low temperature PL measurement, a quartz cuvette containing the Ar-saturated solution of the Ir(III) complex was tightly sealed in Ar-atmosphere. Then the cuvette was inserted into a cryostat (Oxford, optistat DN), and the temperature was controlled with liquid nitrogen. Excitation pulse of 355 nm was generated from the third harmonic output of a Q-switched Nd:YAG laser. The time duration of the excitation pulse was ca. 6 ns. The emission light was collimated before entering monochromator slit and then spectrally resolved by using a 15 cm monochromator (Acton Research, SP150) equipped with a 600 grooves/mm grating after passing the sample. The spectral resolution was about 3 nm for transient photoluminescence experiment. The light signal was detected via a gated ICCD (1024×256). All X-ray data were collected with the use of a Bruker Smart APEX2 diffractometer equipped with a Mo X-ray tube. Collected data were corrected for absorption with SADABS based upon the Laue symmetry by using equivalent reflections.² All calculations were carried out with SHELXTL programs.³

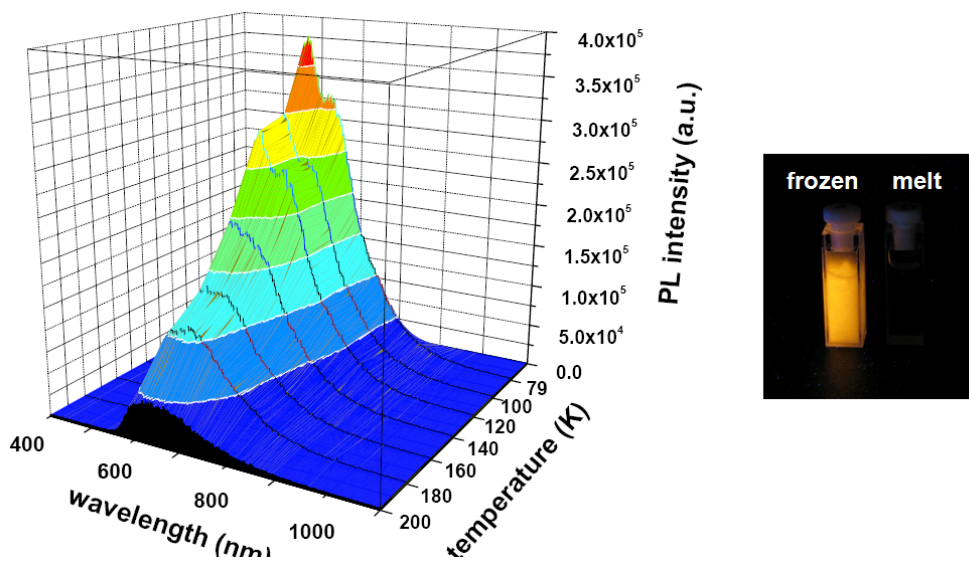
Calculation. Gaussian03 (Gaussian Inc.)⁴ was used for TD-DFT and UCIS calculations. Transition energy was predicted with time-dependent density functional theory (TD-DFT); based on the crystal structure geometry, a “double-ζ” quality basis set of lanl2dz for Ir atom and 6-31G** basis for other atoms was applied together with b3lyp functional. Typically, the lowest 10 triplet and singlet states were obtained. The lowest triplet excited state geometry was determined with UCIS calculation whose starting geometry had been extracted from the single crystal structure.



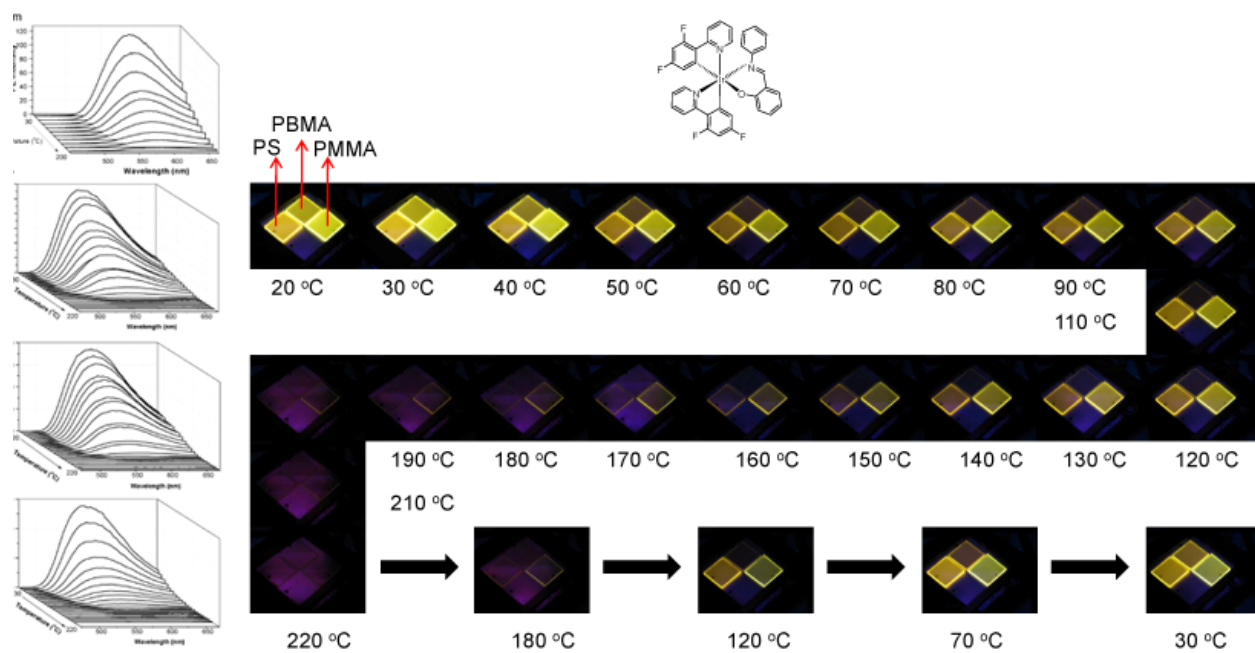
SI 1. Absorption and phosphorescence spectra of 2–4.



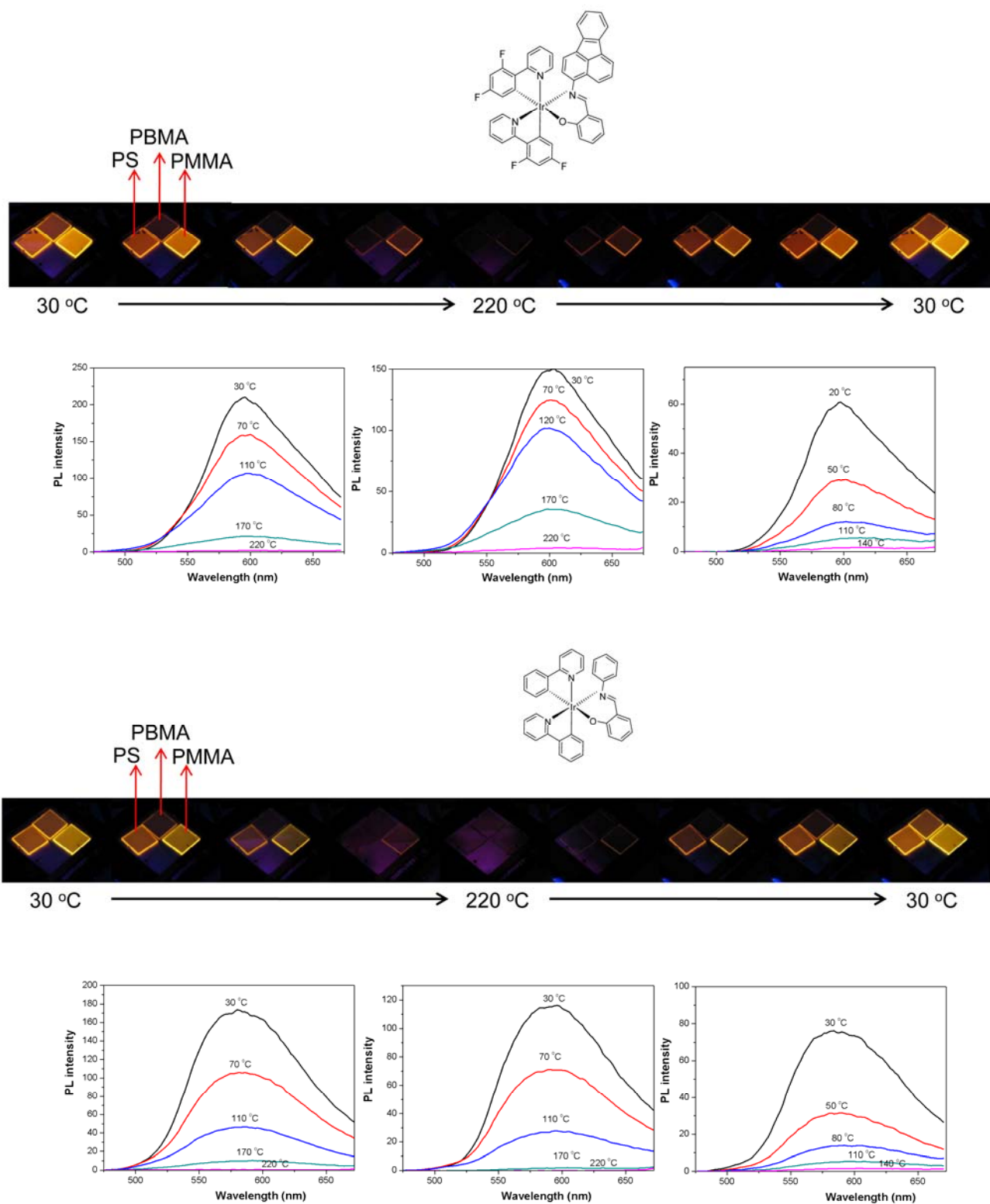
SI 2. Comparative view of the absorption (CH_2Cl_2 , 10 μM) and phosphorescence (PMMA film, 2 wt%) spectra of 1–4.

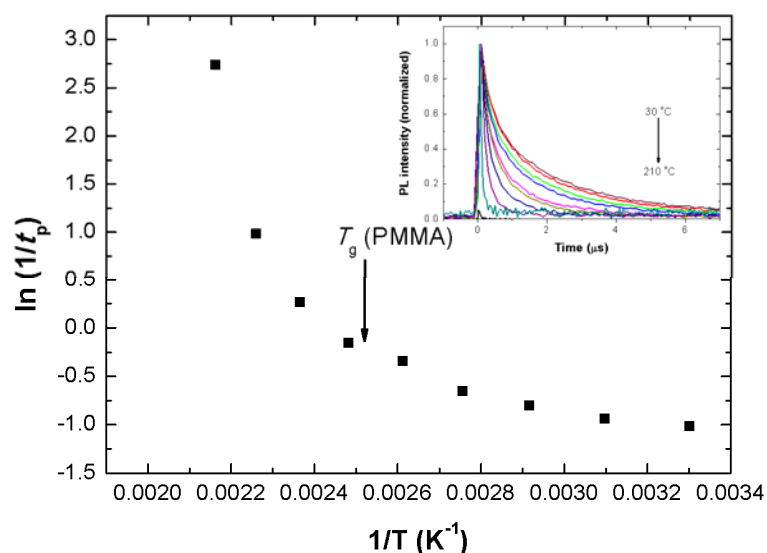


SI 3. Evolution of phosphorescence spectra of 1 (CHCl_3 , 10 μM) as a function of temperature. Left photo: phosphorescence of a frozen and melt solution of 1 in *t*-BuOH (10 μM).

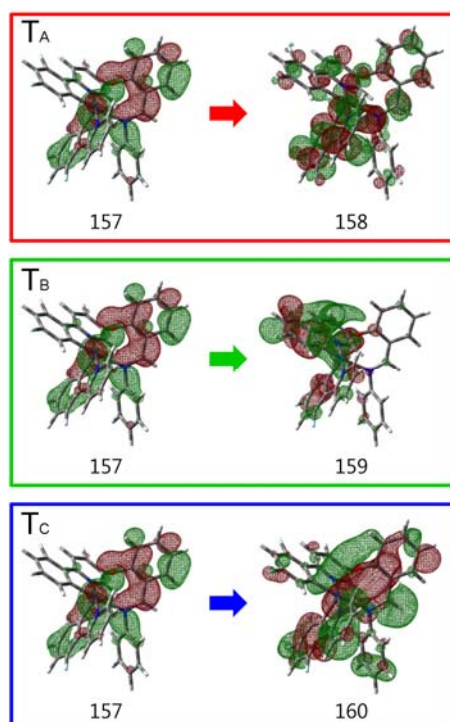


SI 4. Change in phosphorescence of the film states of **1** (left) of neat film, PMMA film (2 wt%), PS film (2 wt%), and PBMA film (2 wt%), respectively (from the top). Right photo is phosphorescence of their films at various temperatures.

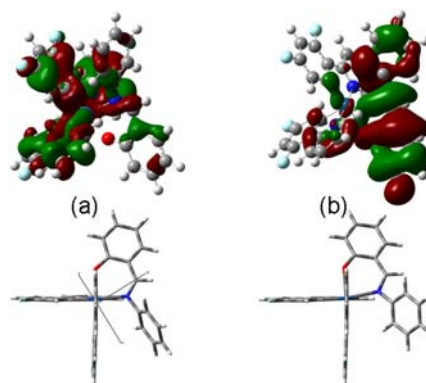




SI 6. A plot of $\ln(1/\tau_p)$ (τ_p : phosphorescence lifetime) as a function of $1/T$ (T : temperature, K) of a PMMA film doped with **1** (2 wt%). Inset figure is decay profiles at various temperatures.



SI 7. Orbital configurations constituting triplet states designated in Fig. 4 of main text. TD-DFT (b3lyp/6-31g**:*lanl2dz*) was applied to a ground state geometry of **1** that was extracted from crystal structure in Fig. 5.



S1 8. (a) LUMO (top, UHF/lanl2dz) and the crystal structure geometry (bottom) of **1**. (b) LUMO (top) and the optimized geometry (bottom) of the triplet state of **1** (UCIS/lanl2dz). Planarization of the N-phenyl ring and resultant change in the orbital distribution is evident in the triplet state geometry.

References

1. A. B. Tamayo, B. D. Alleyne, P. I. Djurovich, S. Lamansky, I. Tsyba, N. N. Ho, R. Bau, M. E. Thompson, *J. Am. Chem. Soc.* 2003, **126**, 7377.
2. G. M. Sheldrick, SADABS, Program for Absorption Correction, University of Göttingen, 1996.
3. Bruker, SHELXTL, Structure Determination Software Programs, Bruker Analytical X-ray Instruments Inc., Madison, Wisconsin, USA, 1997.
2. Frisch, M. J.; Trucks, G. W.; Schlegel, H. B.; Scuseria, G. E.; Robb, M. A.; Cheeseman, J. R.; Montgomery, J. A., Jr.; Vreven, T.; Kudin, K. N.; Burant, J. C.; Millam, J. M.; Iyengar, S. S.; Tomasi, J.; Barone, V.; Mennucci, B.; Cossi, M.; Scalmani, G.; Rega, N.; Petersson, G. A.; Nakatsuji, H.; Hada, M.; Ehara, M.; Toyota, K.; Fukuda, R.; Hasegawa, J.; Ishida, M.; Nakajima, T.; Honda, Y.; Kitao, O.; Nakai, H.; Klene, M.; Li, X.; Knox, J. E.; Hratchian, H. P.; Cross, J. B.; Bakken, V.; Adamo, C.; Jaramillo, J.; Gomperts, R.; Stratmann, R. E.; Yazyev, O.; Austin, A. J.; Cammi, R.; Pomelli, C.; Ochterski, J. W.; Ayala, P. Y.; Morokuma, K.; Voth, G. A.; Salvador, P.; Dannenberg, J. J.; Zakrzewski, V. G.; Dapprich, S.; Daniels, A. D.; Strain, M. C.; Farkas, O.; Malick, D. K.; Rabuck, A. D.; Raghavachari, K.; Foresman, J. B.; Ortiz, J. V.; Cui, Q.; Baboul, A. G.; Clifford, S.; Cioslowski, J.; Stefanov, B. B.; Liu, G.; Liashenko, A.; Piskorz, P.; Komaromi, I.; Martin, R. L.; Fox, D. J.; Keith, T.; Al-Laham, M. A.; Peng, C. Y.; Nanayakkara, A.; Challacombe, M.; Gill, P. M. W.; Johnson, B.; Chen, W.; Wong, M. W.; Gonzalez, C.; Pople, J. A. Gaussian 03, Rev C.02, Gaussian, Inc., Wallingford CT, 2004.